International Journal of Architectural, Civil and Construction Sciences
ISSN: 2415-1734
Vol:13, No:3, 2019

Metallurgical Analysis of Surface Defect in Telescopic Front Fork

Souvik Das, Janak Lal, Arthita Dey, Goutam Mukhopadhyay, Sandip Bhattacharya

***Abstract*—**Telescopic Front Fork (TFF) used in two wheelers, mainly motorcycle, is made from high strength steel, and is manufactured by high frequency induction welding process wherein hot rolled and pickled coils are used as input raw material for rolling of hollow tubes followed by heat treatment, surface treatment, cold drawing, tempering, etc. The final application demands superior quality TFF tubes w.r.t. surface finish and dimensional tolerances. This paper presents the investigation of two different types of failure of fork during operation. The investigation consists of visual inspection, chemical analysis, characterization of microstructure, and energy dispersive spectroscopy. In this paper, comprehensive investigations of two failed tube samples were investigated. In case of Sample #1, the result revealed that there was a pre-existing crack, known as hook crack, which leads to the cracking of the tube. Metallographic examination exhibited that during field operation the pre-existing hook crack was surfaced out leading to crack in the pipe. In case of Sample #2, presence of internal oxidation with decarburised grains inside the material indicates origin of the defect from slab stage.

***Keywords*—**Telescopic front fork, induction welding, hook crack, internal oxidation.

I. Introduction

THE most common form of front suspension for a modern motorcycle is the TFF, see Fig. 1. The front fork is essentially a large hydraulic shock absorber with internal coil springs. The fork assembly connects motorcycle's front wheel and axle to its frame, typically via a pair of triple clamps. The front fork prevents excessive weight on the front wheel during sudden application of the brake and softens bumping when driving on rough road surfaces. The fork assembly mainly contains fork tubes and suspension components (coil springs and damper) which allow steering of the bike through handle bar attached to the top clamp. Springs not only hold up the bike and support both the static load of the bike and the rider, but are also sized or rated to accommodate expected bump loads.

The front fork tube is manufactured from structural grade steel and it attributes high strength, surface finish, ease of manipulation, and closer dimensional tolerance. Initially the coil is loaded on the lock side of double mandrel un-coiler (DMU) by a cantilever crane, and the strap is being cut out manually, followed by straightening of the end of the coil material by pinch roll flattener, only the ends are levelled for coil end welding. Then, the ends of the coils are welded by MIG welding procedure. Then, the strips are accumulated vertically on a larger radius in continuous coil accumulator (CCA). Then, the coil is pickled and pickled slit coils are fed at tube mills for manufacturing tube. The continuous strip coming out of stamping unit is formed to a tubular shape in tube mill. The forming of the strip is initiated by a special w-pass roll drive followed by four pairs of horizontal– vertical rollers. Ultimately fin-pass is used to precise the weld bead thickness. Continuous high frequency induction (HFI) welding takes place, and the tubular-shaped strip is properly formed into a tube. The HFI welding method utilizes pressure and heat in order to join the strip edges of the open seam tube together without the addition of a filler metal. Converging strip edges are pushed against each other by shaped squeezed and pressure rolls in the welding stand. The welding current is introduced into the open seam tube by inductive means using multi-wind coils. The tube welding machine operates constantly at a speed of 80-90 m/min. Then, the pipe passes through roller hearth furnace for normalizing at 880-900 °C. Then, surface treatment is carried out on the tubes followed by cold drawing. Tubes are again put inside the roller hearth furnace to temper them at around 600±20 °C. The tubes are passed through a pair of cooling troughs. These tubes are manufactured along with some tolerance to put them in the required production size. Non-destructive testing (NDT) is carried out to check any sort of failure in the parent material as well as weld crack and surface defects. The defect products are rejected instantly. The manufactured tubes in run out table (ROT) unit run through a series of roll conveyors up to the inspection unit and cooled down in the path. The first part of the unit accepts or rejects a tube as per programmed sensors. Next part consists of a pneumatic air pressure chamber, cleans trimmed parts of the tubes. Finally, the tubes coming out of the inspection chamber are stored aside for some time, then as per the requirement, the tubes are sent to annealing/ normalizing section or hydraulic testing section or dispatched as it is. Schematic diagram of the detailed process is shown in Fig. 2.

The two-wheeler industry has been witnessing double digit growth over the last couple of years. This is reflected in higher production of motorcycles, leading to the demand of TFF tubes growing in recent times. Whereas failure of TFF tubes during production leads to huge damage and decrease the productivity. The present work has been focused on analysis of two different cases related to surface defect of TFF tubes.

Souvik Das, Arthita Dey, Goutam Mukhopadhyay and Sandip Bhattacharya are with the R&D and Scientific Services, Tata Steel Limited, Jamshedpur 831 001, India (e-mail: souvik.das@tatasteel.com).

Janak Lal is with the Product Technology Group, Tata Steel Limited, Jamshedpur 831 001, India.

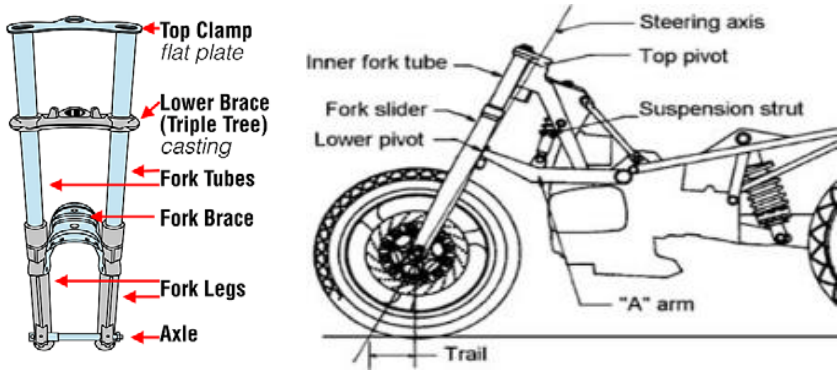

Fig. 1 Schematic view of TFF of motorcycle

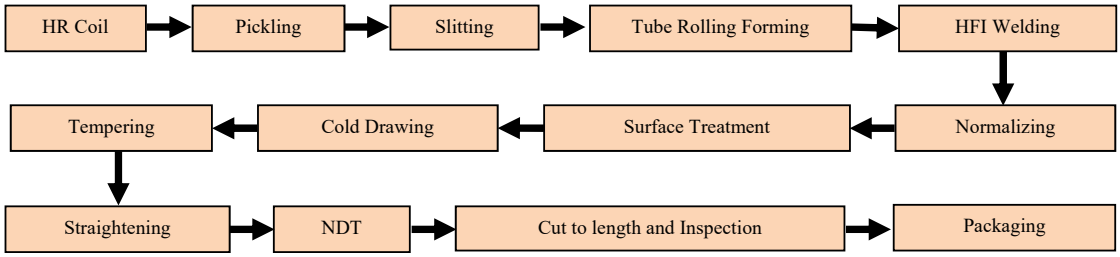

Fig. 2 Schematic diagram of TFF production chain

TABLE I
PARTICULARS OF FAILED SAMPLES

Sl. No.	Type	C	Mn	S	P	Si	Al	N (ppm)	Size (mm)
1	Tube	0.40	1.42	0.010	0.033	0.170	0.052	52	31.10 * 3.55
2	Sample	0.39	1.40	0.006	0.022	0.227	0.015	57	41.28 * 3.80
Spec.	**SAE 1541**	**0.36/0.44**	**1.35/1.65**	**0.05 max**	**0.04 max**	**----**	**----**	**----**	**----**

II. EXPERIMENTAL PROCEDURE AND RESULTS

A. Sample Characteristics

Two failed tube samples were collected from the drawing mill for investigations. The samples were cleaned with acetone to remove dirt for visual examination prior to metallographic sample preparation. Transverse and longitudinal specimens were made from the surface defect location of each failed tube samples for conducting light optical microscopic examination. These samples were individually mounted in conductive mounting and polished by conventional metallographic techniques for scratch free surface. The polished samples were etched in 3% nital solution (3 mL HNO_3 in 97 mL ethyl alcohol), and both un-etched and etched samples were examined in a light microscope to observe microstructural constituents. The micro hardness of different phases observed in the tube samples was determined in a pneumatically controlled automatic micro hardness tester (Leco-$LM247_{AT}$). An applied load of 100gf was used during testing, and several indentations were made to determine the hardness of different phases. Field Emission Gun Scanning Electron Microscope (FEG-SEM) study of the samples was also carried out to identity exact phases present in the samples. The analyses were performed at 15 keV accelerating voltage and 5^{10-8} A probe current.

B. Chemical Analysis

Chemical analysis of samples was carried out using x-ray fluorescence (XRF) spectroscopy except C and S. The carbon (C) and (S) contents were analyzed by combustion infrared technique. All the materials conformed to SAE1541 structural grade with high 'Mn' and low 'S' content. Details of the sample are given in Table I.

C. Visual Observation

Sample #1: Visual observation of the failed fork showed small longitudinal crack along the length of the tube at the circumference close to the weld (Figs. 3 (a) and (b)). The crack was about 4 cm in length and very thin and difficult to detect easily. Crack was very shallow in depth and difficult to detect, so it was detected by dye penetration test (Figs. 3 (c) and (d)).

Sample #2: General view of the tube sample with defect is shown in Fig. 4 (a). Multiple chevron marks were observed on the surface of the tube. These chevron marks were found to form a single line (Figs. 4 (a) and (b)). Similar marks with less severity and a line mark running through centre of these defects were observed at 180-degree location (Fig. 4 (a)).

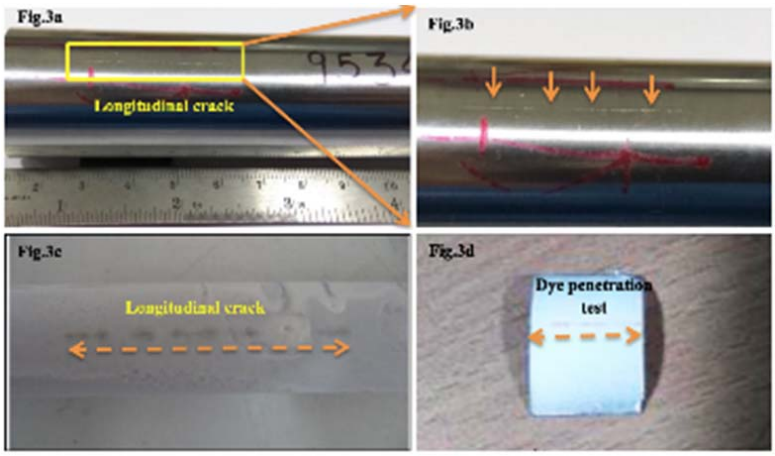

Fig. 3 (a) and (b) Longitudinal crack along the length of the tube, longitudinal crack was detected through dye penetration test

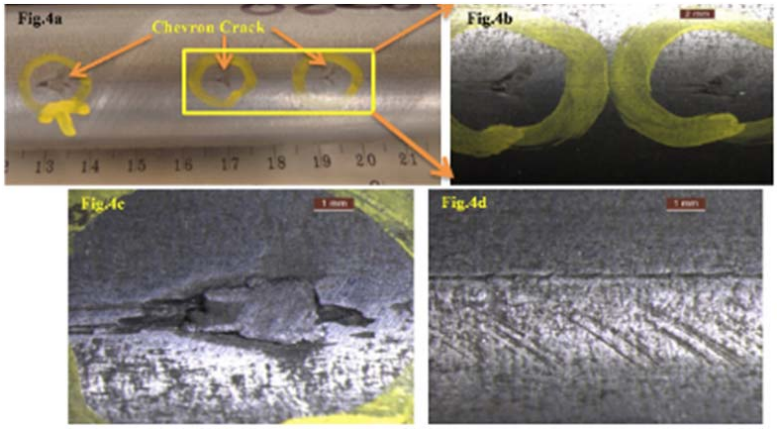

Fig. 4 (a)-(c) Chevron cracks on the surface of the tube, (d) Less severity defects were observed at 180-degree location of the chevron crack

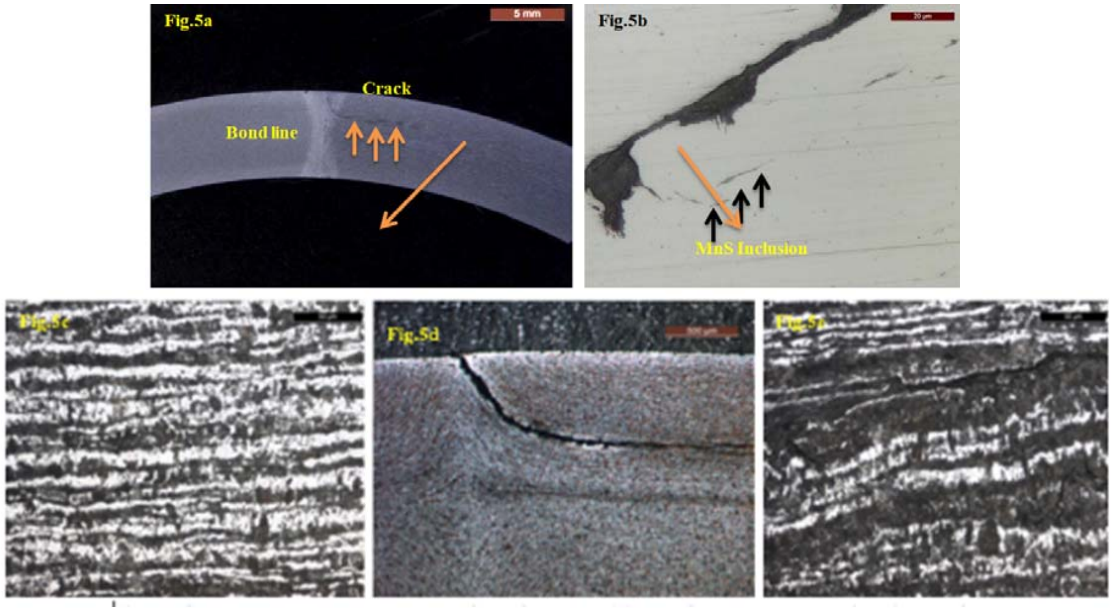

Fig. 5 (a) Chevron cracks on the surface of the tube, (b) Un-etched micro image of the defect location, (c)-(e): Etched micro image of the defect location at different magnifications

D. Microstructure Analysis

Sample #1: The un-etched microstructure showed a crack, 'J' type in shape and of 0.5 mm in depth (Fig. 5 (a)), typical to hook cracking [1]. Further the crack was found to be associated with some non-metallic manganese sulfide (MnS) inclusions (Fig. 5 (b)) which were further conforms through EDS analysis. The macro dual zoom photograph of the micro sample revealed white bond line associated with the crack (Fig. 5 (c)). The 3% nital etched microstructure showed that the crack was slightly offset from the bond line of the Cold drawn Electric resistance Welding (CEW) seam (Fig. 5 (a)), but following the weld flow lines and opened up at the circumference. The hook of the crack turned toward upward, as shown in Fig. 5 (d). The weld flowline of the tubes was compatible to the cold drawn structure (Fig. 5 (d)), and the matrix revealed banded ferrite pearlite structure (Figs. 5 (c) and (e)) common to such high manganese structural steel grades [2].

Sample #2: Un-etched micro image of the samples from defect area revealed bowl shaped defect. This was formed by chipped-off material as shown in Fig. 6 (a). Figs. 6 (b) and (c) show closer view of the cracks on both edges of the defect. It can be observed that the cracks contain some non-metallic entrapments in it. At higher magnification, as shown in Fig. 6 (e), suspected internal oxidation can be observed in chipped-off material.

The etched microstructure at the defect location is shown in Fig. 7 (a). Banded ferrite - pearlite structure was observed which followed the contours of the defect/chipped-off material. At higher magnification, decarburised grains were observed along the suspected internal oxidation. The chipped-off material does not show any banding or deformation. However, due to accumulation of this material, grains in the matrix below, it got deformed which is cold condition effect.

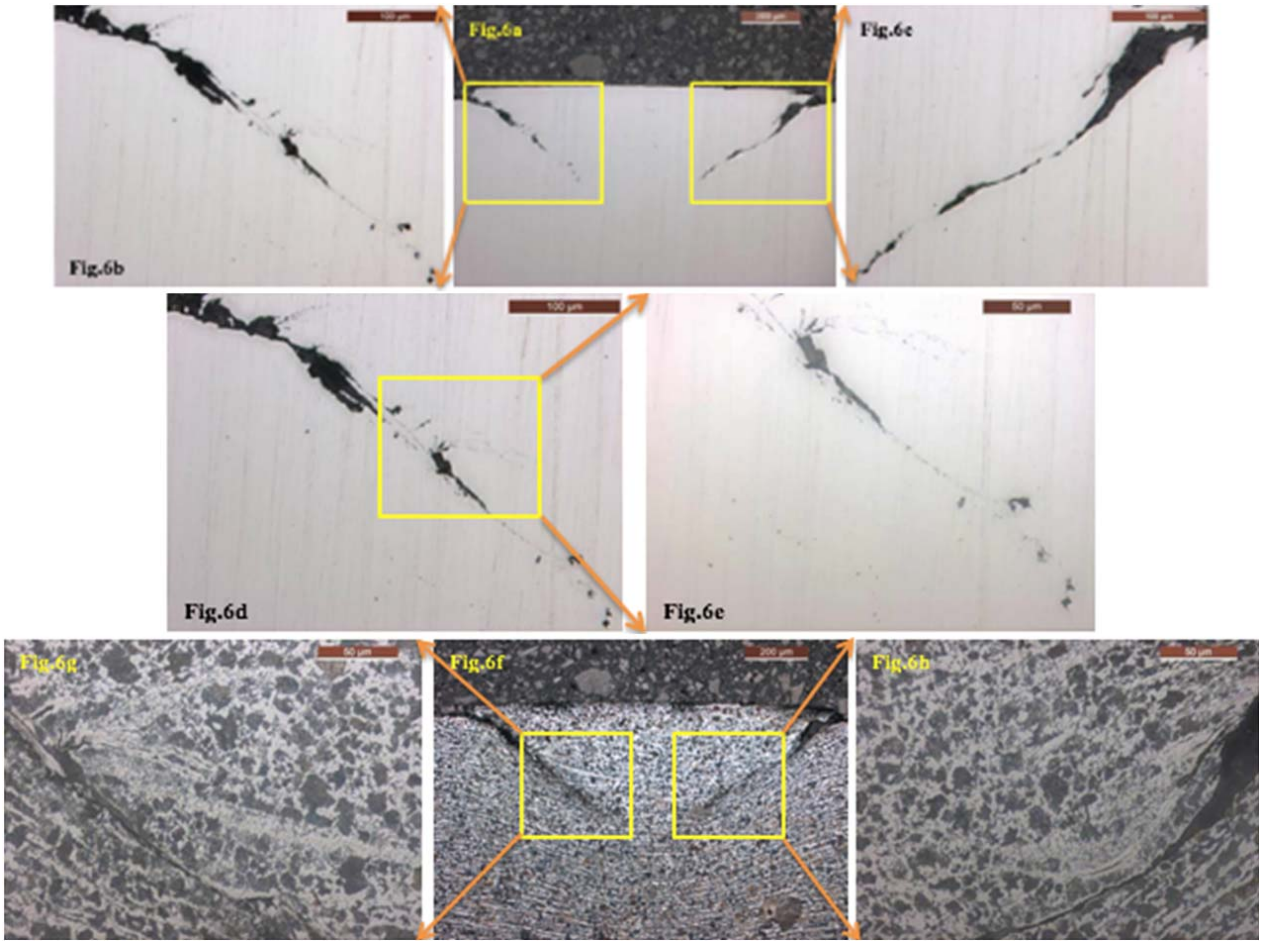

Fig. 6 (a)-(d) Un-etched micro image of the defect location at different magnifications, (e) Presence of dark brown entrapment along with internal oxidation (f)-(h) Etched micro image of the defect location at different magnifications

E. SEM and EDS Analysis

Sample #1: EDS analysis was carried out on non-metallic inclusion by Scanning Electron Microscope at an accelerating voltage of 15 kV. EDS analysis conformed the inclusions as MnS (Fig. 7 (a), Table II). Then, inclusion rating was also carried out by ASTM E 45 method to check overall cleanliness of the steel. The inclusion rating, shown in Table III, revealed higher MnS inclusions in steel.

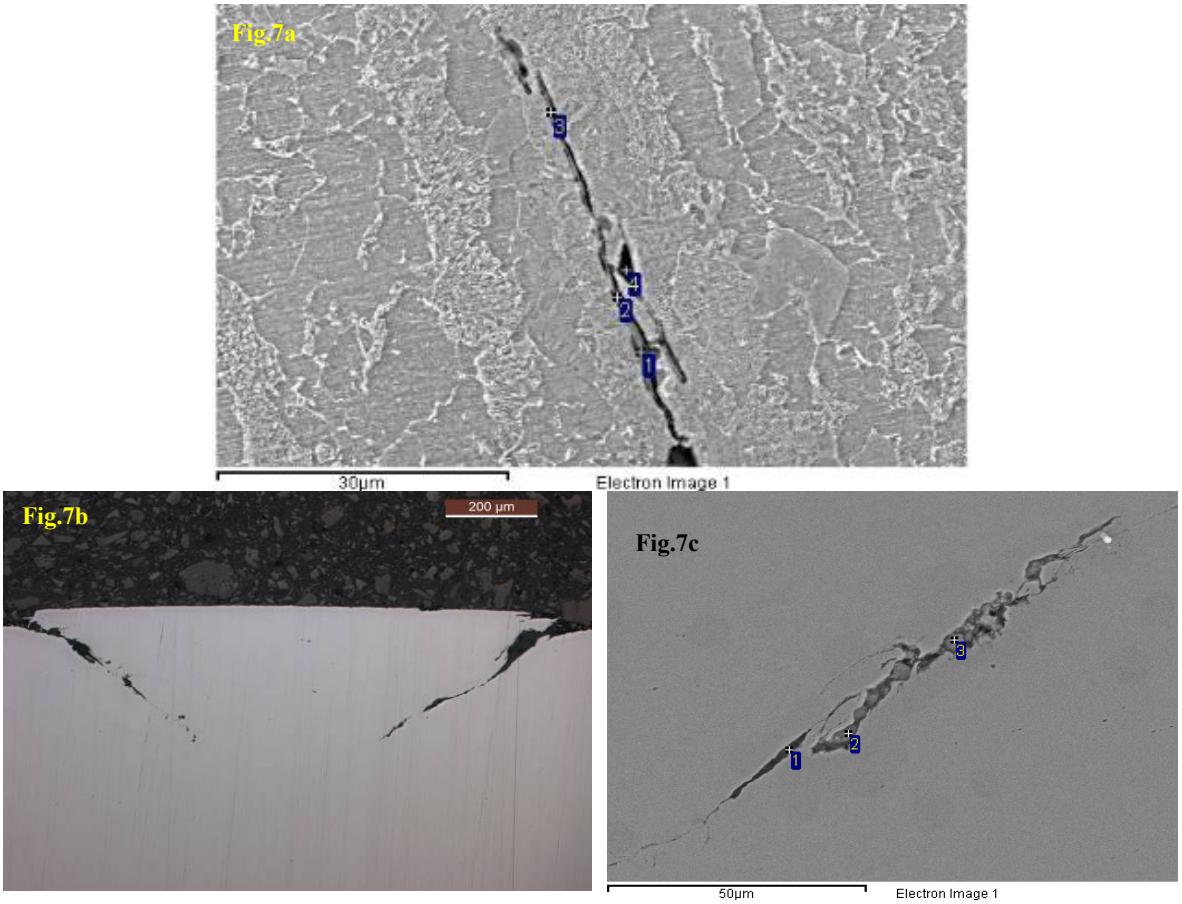

Fig. 7 (a) EDS analysis of sample#1 at cracked location, (b) and (c) EDS analysis of sample#2 at defect location

TABLE II
EDS ANALYSIS OF SAMPLE#1

Sl. No.	Chemical composition (wt. %)					
	O	P	S	Ti	Mn	Fe
1	4.22	0.32	20.79	0.38	38.83	35.46
2	3.82	0.44	15.75	0.36	26.98	52.65

TABLE III
INCLUSION RATING OF SAMPLE#1

Sample No.	Inclusion rating (ASTM E-45)			
	A(T/H)	B(T/H)	C(T/H)	D(T/H)
1	1.5 / 0.0	0.0 / 0.0	0.5 / 0.0	0.5 / 0.0

TABLE IV
EDS ANALYSIS OF SAMPLE#2

Sl. No.	Chemical Composition (Wt. %)						
	O	F	Na	Al	Si	Ca	Fe
1	22.44	4.94	4.66	2.92	10.41	16.52	38.11
2	10.28	4.52	3.9	2.09	7.11	11.66	60.43
3	17.5	1.88	8.8	7.0	10.4	5.78	48.65

Sample #2: EDS analysis of the dark brown entrapment revealed prominent peaks of Ca, Si, Al, Na, F and O which proves that crack has generated due to mould powder entrapment.

III. DISCUSSION

Sample #1: Visual observation of the failed fork tube showed presence of small cracks along the length of the tube at the circumference adjacent the weld flow lines. The crack was about 5 cm in length. The unetched microstructure of crack showed 'J' type hook crack [1], [2]. MnS inclusions were observed in the vicinity of the crack. The overall MnS inclusion was high as shown in Table III. Microstructural analysis further revealed that the hook of the crack was turning toward upward surface. The originator of hook crack is non-metallic inclusion primarily MnS stringers. These flattened non-metallic inclusions are formed during hot rolling of plate. They reduce the ductile toughness of the steel even in their normal position but do not affect the yield or tensile strength of the steel [3]. So, the mechanical properties of the tube under investigation were also satisfactory. Near bondline, these weak layers reorient themselves in such a way that they become subjected to tensile hoop stress when the pipe is pressurized [4] and a small crack originates. The slight upset of the metal at the weld acted to turn the ends of this usually very small subsurface crack in the direction of the upset. Because the metal flow during the upset is toward the both surfaces. The hook of the hook crack may turn toward either the outside or inside surface, depending on which the

delamination takes place in that direction where, the greatest amount of upset occurs. Generally the upset is greater toward the outer surface this causes the hook to turn towards outer surface [5]. In current investigation, also the crack turned toward the outer surface due to greater upset toward the outer surface. Since hook cracks are observed in the plate thickness, therefore surface oxidation through hot rolling and heat treatment cannot be responsible for hook crack [6]. The chemical composition of the sample showed higher high manganese and sulfur ratio and in this case favored the formation of MnS inclusion resulted in higher inclusion rating. These MnS inclusions caused imperfection at the edge of the strip which turned toward the outside diameter pipe surface resulting in hook crack formation during upsetting at the time of welding. Thus, the hook crack was originated during tube manufacturing which surfaced out when the tube was put in field service.

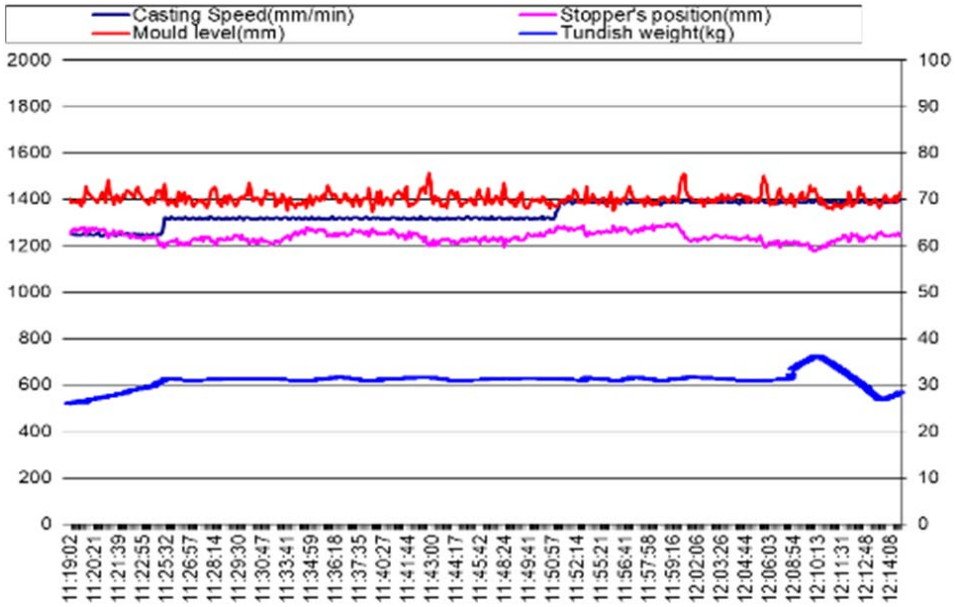

Fig. 8 Casting parameters for sample #2

Sample #2: Repeating chevron marks were observed to form a single line at certain interval on the tube surface. Similar marks with less severity and a line mark running through centre of these defects were observed at 180-degree location. Closer observation of the chevron marks in stereo microscope shows accumulation of material at centre of the chevron. Optical microscopy shows grain deformation at the defect contour indicating cold stage deformation. Based on the repetitive nature of the defect, it appears to be originating from the drawing stage itself and that too at exactly diametrically opposite locations of the tube. Decarburised grains along with internal oxidation associated with dark brown entrapment were observed along the cracks. Presence of mould power entrapment inside the material indicates origin of the defect from slab stage. The morphology and location on the tube suggests that the steel defect got aggravated during drawing forming the chevron mark. Mold powder entrapment mainly occurs in the so-called ‘‘transient casting’’ periods, e.g. the time of casting start, casting end, ladle exchange, mold width change, SEN change, etc. During the unsteady casting periods, usually, the casting speed is largely varied, which disturbs the flow of the liquid steel in the mold and results in severe level fluctuation. Hence, mold powders are easy to be carried into the liquid steel, and some are entrapped by the solidified shell and exist as non-metallic inclusions in slabs. If the interfacial velocity of steel melt which exceeds tear off velocity results in associated shear stress to become greater than the cohesion forces of the slag. Slag gets torn off and carried over in the form of droplets in the liquid metal. While a part of these droplets immediately floats back towards the meniscus, another part is transported by the metal flow and scattered in the liquid pool [7]. In case of sample #2, it has been observed that higher severity index in this coil is explained due to unstable stopper position shown in the caster (Fig. 8). As seen from the chart given for this slab, there are large fluctuations in casting speed along with large mold level fluctuations. Hence, changing stopper position causes unstable molten steel flow and so entrapment of mold powder.

IV. Conclusion

In case of Sample #1: Analysis of the results suggests that the presence of MnS inclusion at the edge of the caused the origin of the hook crack, which exposed to the surface under cyclic mode in field operation, resulting in cracking of the telescopic fork tube.

In case of Sample #2: The slag entrapments of the mold fluxes in sub-surface of the strands are the main origin of the surface defect in telescopic fork tube. The morphology and

location on the tube suggests that the steel defect got aggravated during drawing forming the chevron mark.

REFERENCES

[1] Quickel, G. T., Rollins, B. C., Beavers, J. A.: Analysis of seam weld related pipeline failures. Mater. Sci. Technol. 8, 514–523 (2008).
[2] Bhadeshia, H. K. D. H., Honeycombe, R. W. K.: Steel Microstructure and Properties, pp. 299–301. Butterworth-Heinemann Publications, Boston (2011).
[3] Koo, J. Y.: Welding Metallurgy of Structural Steels, p. 574. Metallurgical Society Inc, Warrendale (1987).
[4] Rick Meade: Report submitted on non-destructive evaluation of low-frequency electric resistance welded pipe utilizing ultrasonic in-line inspection technology, Tubesscope Pipeline Services, Houston (2006).
[5] ASM Hand-Book, vol. 11—Failure Analysis and Prevention, p. 191, 2005.
[6] Arthita Dey, Sharmistha Dhara,Tanmay Bhttacharyya,Sandip Bhattacharyya: Cracking of Telescopic Front Fork Tube During Field Operation, J Fail. Anal. and Preven. (2013) 13:292–297.
[7] Souvik Das, Shomick Roy, Soumilya Nayak, Tanmay Bhattacharyya, Sandip Bhattacharyya: Case study – Analysis of grayish stick type sliver in cold rolled Strips; Engineering Failure Analysis 44 (2014) 95–99.